remote sensing

MDPI

Article

Analyzing and Predicting LUCC and Carbon Storage Changes in Xinjiang's Arid Ecosystems Under the Carbon Neutrality Goal

Jie Song [1,†], Xin He [1,†], Fei Zhang [2,*], Xu Ma [1], Chi Yung Jim [3], Brian Alan Johnson [4] and Ngai Weng Chan [5]

[1] College of Geography and Remote Sensing Sciences, Xinjiang University, Urumqi 830017, China; 107556522164@stu.xju.edu.cn (J.S.); rshexin@stu.xju.edu.cn (X.H.); maxu2020@xju.edu.cn (X.M.)
[2] College of Geography and Environmental Sciences, Zhejiang Normal University, Jinhua 321004, China
[3] Department of Social Sciences and Policy Studies, Education University of Hong Kong, Tai Po, Hong Kong 999077, China; cyjim@eduhk.hk
[4] Natural Resources and Ecosystem Services Area, Institute for Global Environmental Strategies, Hayama 2400115, Kanagawa, Japan; johnson@iges.or.jp
[5] GeoInformatic Unit, Geography Section, School of Humanities, University Sains Malaysia, Penang 11800, Malaysia; nwchan@usm.my
* Correspondence: zhangfei3s@zjnu.edu.cn
† These authors contributed equally to this work.

Abstract: Land use/cover change (LUCC) significantly alters the carbon storage capacity of ecosystems with a profound impact on global climate change. The influence of land use changes on carbon storage capacity and the projection of future carbon stock changes under different scenarios are essential for achieving carbon peak and neutrality goals. This study applied the PLUS-InVEST model to predict the land use pattern in China's arid Xinjiang Region in 2020–2050. The model assessed the carbon stock under four scenarios. Analysis of the historical LUCC data showed that the carbon storage in Xinjiang in 2000–2020 in five-year intervals was 85.69×10^8, 85.79×10^8, 85.87×10^8, 86.01×10^8, and 86.71×10^8 t. The rise in carbon sequestration capacity in the study area, attributable to the expansion of cropland, water, and unused land areas, brought a concomitant increment in the regional carbon storage by 1.03×10^8 t. However, prediction results for 2030–2050 showed that carbon storage capacity under the four scenarios would decrease by 0.11×10^8 and increase by 1.2×10^8, 0.98×10^8 t, and 1.28×10^8 t, respectively. The findings indicate that different land transfer modes will significantly affect Xinjiang's carbon storage quantity, distribution, and trend. This research informs the past, present, and future of carbon storage in arid ecosystems of Xinjiang. It offers a reference for Xinjiang's development planning and informs the efforts to achieve the carbon peak and neutrality goals.

Keywords: LUCC; CA-Markov; PLUS-InVEST; multi-scenario simulation; carbon storage; carbon peak and neutrality

Citation: Song, J.; He, X.; Zhang, F.; Ma, X.; Jim, C.Y.; Johnson, B.A.; Chan, N.W. Analyzing and Predicting LUCC and Carbon Storage Changes in Xinjiang's Arid Ecosystems Under the Carbon Neutrality Goal. *Remote Sens.* **2024**, *16*, 4439. https://doi.org/10.3390/rs16234439

Academic Editor: Jean-Christophe Calvet

Received: 17 October 2024
Revised: 10 November 2024
Accepted: 22 November 2024
Published: 27 November 2024

1. Introduction

Land use and cover changes (LUCC) significantly contribute to global warming by influencing the carbon cycle within terrestrial ecosystems [1–3]. Carbon storage, a critical ecosystem service, is a key indicator of the impacts of global climate change on terrestrial ecosystems [4]. Enhanced carbon storage reduces atmospheric CO_2, thereby mitigating the greenhouse effect and contributing to the regulation of global climate [5]. LUCC is recognized as a primary factor shaping carbon storage levels due to its impact on ecosystem structure and function [6]. Consequently, the study of land use change has become a central approach in examining the impacts on terrestrial ecosystems [7].

LUCC is a major driver of various regional and global environmental processes, including disruptions to the terrestrial carbon cycle, which is intricately linked to climate change research. Its effects on global carbon cycling, atmospheric CO_2 concentrations, and climate change necessitate detailed investigations [8–10]. Land use transformations and the resultant land use configurations principally influence the capacity of vegetation and soils to sequester carbon. A reduced sequestration potential leads to the degradation of this vital ecosystem service [11,12]. LUCC can alter ecosystem structure and function in ways that affect carbon storage, reflecting global climate change trends. Disruptions to the carbon cycle due to LUCC can depress the benefits of carbon storage, such as reducing atmospheric CO_2 and mitigating climate change [13,14].

China has set a strategic objective to achieve its dual carbon goals (peak and neutrality), which are integral to the nation's socio-economic development. Augmenting carbon storage in terrestrial ecosystems has been extensively researched across various academic fields [15,16]. Insights from these studies enhance our understanding of human influences on carbon dynamics and support efforts to reduce carbon emissions. In this context, provincial and municipal governments in China are actively seeking ways to achieve coupled source–sink targets. They include evaluating the impacts of LUCC on carbon storage to decrease carbon emissions in Xinjiang, located in the country's arid northwest region [17]. Protecting natural forest and grassland ecosystems is essential for maintaining their capacity to capture atmospheric CO_2 through photosynthesis and storage in biomass [18]. A comprehensive analysis of LUCC can optimize regional development potential by optimizing land use structure, enhancing ecosystem services, and mitigating climate change impacts.

The research on land use impacts spans various scales, covering national, provincial, and municipal levels. These studies often focus on humid/semi-humid climates and economically developed regions, examining LUCC spatiotemporal characteristics [19,20], LUCC drivers [21], ecological values of land use [22], and landscape patterns [23]. The latest CMIP6 climate change model offers a range of future scenarios for global climate change [24,25]. Relevant studies have assessed carbon storage in some parts of China by modeling various scenarios. These studies have explored variations in LUCC and carbon storage under different development models by integrating land use prediction models with the InVEST model [26]. Land use prediction models, such as the PLUS model, have the advantage of applying cellular automata to deeply investigate land use changes in order to more accurately simulate complex evolutionary processes of multiple land classes [27]. The InVEST (Integrated Valuation of Ecosystem Services and Trade-offs) model estimates changes in the quantity and value of ecosystem services based on land use data, providing a scientific basis for quantifying the benefits and impacts of human activities [28]. Based on these methods, Li et al. [29] evaluated the spatiotemporal characteristics of carbon storage in the past 20 years. They predicted land use changes and effects on carbon storage under three scenarios for 2050. He et al. [30] applied the PLUS and InVEST models to quantify the carbon storage and spatial distribution in Guilin. They found that high-carbon-storage regions were mainly located in the northeast and northwest of the study area. Zhu et al. [31] used the PLUS-InVEST model to simulate the trajectory of carbon storage changes in Hunan Province from 2000 to 2020 under various scenarios, demonstrating high accuracy in their land use forecasting. Similarly, Yu et al. [32] employed the CA and PLUS models to project changes in ecosystem carbon storage in the Beijing–Tianjin–Hebei region under distinct development scenarios from 2030 to 2060, incorporating a carbon density table for vegetation types. Their study demonstrated that the remote sensing monitoring of land use changes improves the understanding of the spatial distribution of carbon storage at large scales, contributing to the carbon balance stabilization of regional ecosystems. Previous studies focused on the impact of land use changes on carbon storage under different development scenarios using land use modeling. However, a research gap exists in China's arid and semi-arid regions with fragile ecological environments. Hence, it is necessary to conduct more research to clarify the spatiotemporal distribution of carbon stocks in arid and semi-arid zones that are more sensitive to climate change, and project future trends. In addition, considering the natural conditions of Xinjiang, such as its vast area, high mountains, and extensive deserts, remote sensing technology can facilitate ecosystem carbon stock estimation and monitoring.

Accordingly, this study simulates the spatiotemporal patterns of carbon storage in Xinjiang under four scenarios using the coupled PLUS-InVEST model. The project aims to (1) analyze the past and present characteristics of LUCC dynamics from 1980 to 2020 at 10-year intervals; (2) predict the LULC (land use/land cover) map for 2050 under four scenarios to assess the distribution of carbon storage in Xinjiang by combining the CA-Markov and InVEST models; and (3) clarify the impact of LULC dynamics on ecosystem carbon stocks in arid zones from 2000 to 2050. The results can inform planning for economic development under different scenarios, balancing ecological and environmental protection. The findings are expected to support decision-making to achieve nature conservation and sustainable development in China's ecologically vulnerable arid regions of the northwest, fostering regional green and low-carbon growth.

2. Materials and Methods

2.1. Study Area

The Xinjiang Uygur Autonomous Region (hereinafter referred to as "Xinjiang") lies in northwest China, in the heart of the large Eurasian land mass (73°29′54″~96°23′3″E, 34°20′11″~49°10′55″N). Situated in China's continental interior (Figure 1), it has a wide seasonal temperature range, low and unevenly distributed precipitation, abundant sunshine, and a high potential evapotranspiration rate. The high mountain ranges function as topographic barriers that hinder water vapor passage to bring a typical temperate continental arid climate [33]. The low vegetation cover and distinct topographic and climatic features lead to significant spatial and altitudinal variations of regional flora. The region is ecologically vulnerable and climate change sensitive. The three major mountain ranges in Xinjiang, Altai, Tianshan and Kunlun, are thousands of kilometers long, running through Central Asia and connecting to South Asia. The region includes large intermontane basins such as Junggar and Tarim and extensive deserts such as Gurbantunggut, Taklamakan, Kumtag, Badain Jaran, and Tengger [34].

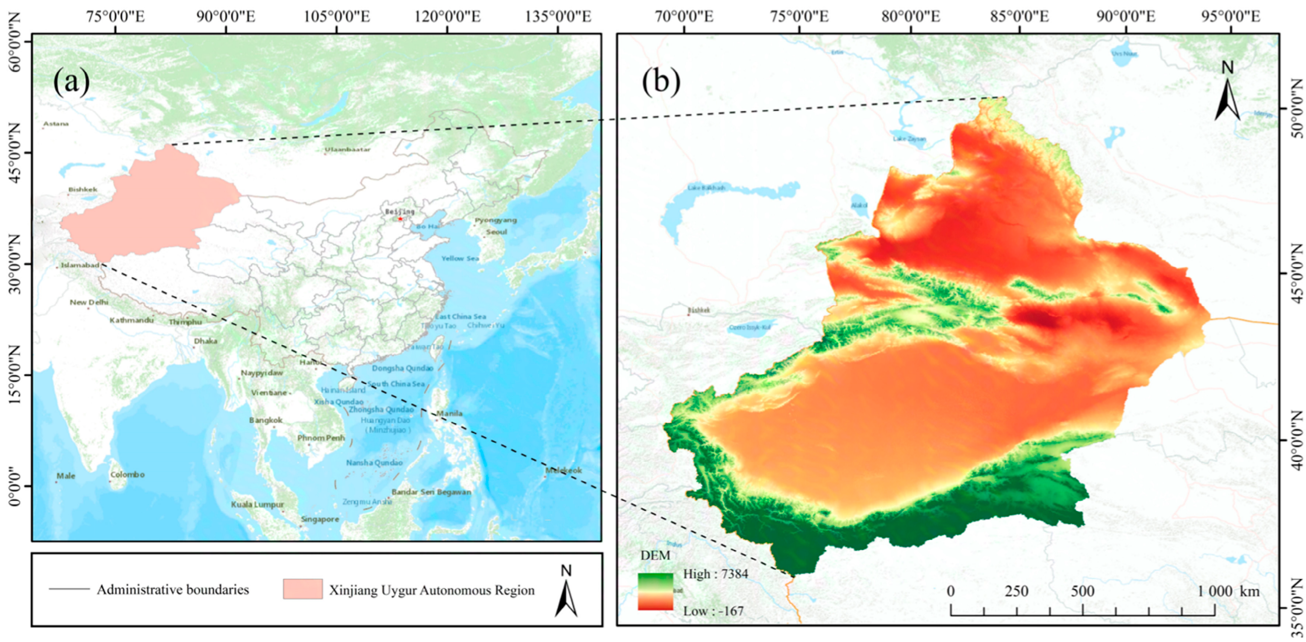

Figure 1. Maps of the study area: (**a**) Geographic location of Xinjiang in China; (**b**) topography of Xinjiang.

2.2. Data Sources and Preprocessing

2.2.1. LULC Driving Data

The LUCC drivers encompassed socio-economic, natural, and accessibility factors. Socio-economic factors comprised GDP representing socio-economic status and population (POP). Natural factors, such as elevation and slope, were extracted from the digital elevation model (DEM). This Supplementary Information includes temperature and precipitation data. The accessibility factor includes proximity to the city and distance to the river, road, railway, and national highway. All map data used in this study were transformed into the Krasovsky 1940 Albers coordinate system (Table 1).

Table 1. Data collection and sourcing.

Driving Factor	Accuracy	Source
Land use	30 m	Data Center for Resources and Environmental Sciences of the Chinese Academy of Science (https://www.resdc.cn/, accessed on 20 April 2024)
Gross domestic product (GDP) Population (POP)	1 km	Data Center for Resources and Environmental Sciences of the Chinese Academy of Science (https://www.resdc.cn/, accessed on 20 April 2024)
Temperature Precipitation Digital elevation model (DEM) Slope	30 m	Geospatial data cloud (http://www.gscloud.cn, accessed on 3 March 2024)
Proximity to city Distance to river Distance to road Distance to railway Distance to national highway	30 m	1:250,000 national basic geographic database (https://www.webmap.cn, accessed on 13 July 2024)

2.2.2. Carbon Density Data

These data were sourced from the National Ecosystem Science Data Center (https://www.cern.ac.cn, accessed on 16 October 2024). They were realized by merging the carbon density of China's terrestrial ecosystems with pertinent experimental data [35]. The dataset provides a comprehensive and structured profile of organic carbon density in vegetation and soil of different ecosystems in Xinjiang (Table 2).

Two methods were used in this study to calculate carbon density data: searching and revising carbon density data in comparable regions using a precipitation correction model [36]. The estimation of carbon density values for water bodies and construction sites, as well as biomass and soil carbon density, was calculated by applying correction factors in conjunction with the effects of precipitation and temperature. The equations for these correction factors are presented below [37,38]. This model is generally suitable for regions with relatively uniform climate conditions; however, adjustments may be needed to fully account for Xinjiang's climatic diversity. Carbon storage in dead organisms was not determined in this survey due to difficulties in data collection and the inherently low carbon storage in dead organisms [39,40]. The exact formula is as follows:

$$C_{BP} = 6.798e^{0.0054MAP}(R^2 = 0.70) \tag{1}$$

$$C_{BT} = 28MAT + 398(R^2 = 0.47, P \leq 0.01) \tag{2}$$

$$C_{SP} = 3.3968MAP + 39996.1(R^2 = 0.11) \tag{3}$$

where C_{BP} and C_{BT} represent biomass carbon density based on mean annual precipitation and mean annual temperature, respectively, and C_{SP} represents soil carbon density. MAP stands for mean annual precipitation, and MAT represents mean annual temperature. The equations for the precipitation and temperature correction factors are:

$$K_{BP} = \frac{C'_{BP}}{C''_{BP}}; K_{BT} = \frac{C'_{BT}}{C''_{BT}}; K_B = K_{BP \times} K_{BT} = \frac{C'_{BP}}{C''_{BP}} \times \frac{C'_{BT}}{C''_{BT}} \quad (4)$$

$$K_S = \frac{C'_{SP}}{C''_{SP}} \quad (5)$$

where K_{BP} represents the precipitation correction factor for biomass carbon density, K_{BT} represents the temperature correction factor for biomass carbon density, K_B represents the correction factor for biomass carbon density, and K_S represents the correction factor for soil carbon density. The data from Xinjiang are denoted by $C^{'}$, and the data from China are denoted by $C^{''}$.

We acquired initial carbon density data on the vegetation and soil of China's cultivated land, forest, and grassland from Xie et al. [41], and cultivated land, forest, and grassland in Xinjiang were sourced from Cui et al. [42]. Below-ground biomass carbon density values for water, construction land, and unused land were assumed to be 0 [43]. The mean annual temperature in China was 9 °C, and in Xinjiang was 8.6 °C. The mean yearly precipitation levels were 628 mm and 150 mm, respectively.

This research obtained land use carbon density data from previous studies and adjusted them with meteorological factors, yielding more accurate outcomes than using national data directly. Variations in carbon density obtained by different studies should be recognized. To minimize discrepancies, the selection of literature sources was carried out very carefully. Where feasible, the same authors were selected when using the data to ensure reliability and scientific rigor. Furthermore, literature data from regions with comparable climate conditions and geographical locations were enlisted. This study selected literature data from China's northern regions and excluded data from southern regions or other countries. Therefore, this study's calculated carbon density values are reasonable and dependable (Table 2). For cross-referencing, our calculated carbon density data are consistent with comparable studies, including Lu et al. [44] in Tianshan Mountains, Wang et al. [45] in cultivated land, Hua et al. [46] in Kanas, Aishan et al. [47] in Tarim River Watershed, Jia et al. [48] in desert, Cui et al. [42] in grassland, and Zhang et al. [49] in arid western China.

Table 2. The carbon density of six land use types in Xinjiang (t/hm^2).

Land Use Type	C_{above}	C_{below}	C_{soil}	Source
Cultivated land	0.46	6.46	83.8	[35,36,41]
Forest	3.39	9.27	131.3	[35,36,50]
Grassland	2.82	6.92	80.0	[35,41,50]
Water	0.01	0	36.8	[36,50,51]
Construction land	0.02	0	71.4	[36,50,51]
Unused land	0	0.65	28.5	[50–52]

2.3. Methods

2.3.1. CA-Markov Model

This model describes the transition probability matrix to simulate prospective LUCC maps over time [53]. The Markov approach illustrates the progression of a system from one state to another, forecasting future changes in an event based on its current status at each moment or period [54]. It is one of the crucial forecasting methods used in geographical research. Assuming that there are n potential states for the predicted event, such as E_1, E_2, . . ., E_n, let P_{ij} represent the state transition probability from state E_i to state E_j, and the matrix is constructed [55]:

$$P_{ij} = \begin{bmatrix} P_{11} & P_{12} & \cdots & P_{1n} \\ P_{21} & P_{22} & \cdots & P_{2n} \\ \vdots & \vdots & \vdots & \vdots \\ P_{n1} & P_{n2} & \cdots & P_{nn} \end{bmatrix} \quad (6)$$

$$S(t+1) = S(t) \times P_{ij} \tag{7}$$

The transition probability matrix P is commonly referred to as the state transition probability matrix. To compute this matrix, we must determine the transition probabilities P_{ij} (where i and j range from 1 to n) for each state to shift to any other state. In order to obtain each P_{ij}, we employ the concept of frequency approximate probability to calculate it.

2.3.2. InVEST Model

This model can estimate the amount of carbon held by different land use types [56]. Four main carbon pools are evaluated: above-ground biomass, below-ground biomass, soil, and dead organic matter. The model estimates the current amount of carbon storage by incorporating LUCC maps and storage values for these carbon pools. Such data can formulate policies and management choices to enhance carbon sequestration and mitigate climate change [57,58]. The equations are:

$$C_i = C_{i\_above} + C_{i\_below} + C_{i\_soil} + C_{i\_dead} \tag{8}$$

$$C_{total} = \sum_{i=1}^{n} C_i \times A_i \tag{9}$$

where C_i represents the average carbon density of land use type i, C_{i_above} represents the above-ground biomass carbon density, C_{i_below} represents the below-ground vegetation carbon density, C_{i_soil} represents the soil carbon density, and C_{i_dead} represents the carbon density of dead organic matter. Additionally, C_{total} represents the total carbon storage, while A_i represents the area of type i.

2.3.3. PLUS Model

The PLUS model is a widely adopted cellular automata (CA) framework for modeling the dynamics of intricate LUCC systems [59]. The model consists of two main modules: LEAS is a transformation rule mining component, and CARS is responsible for generating land use patches [60]. Meanwhile, the CARS module functions as a cellular automata (CA) tool that simulates spatial alterations under complex scenarios by influencing local competition for land use to satisfy future demands [61].

2.3.4. Defining Development Scenarios

CLP (cultivated land protection): This policy analysis model focuses on cultivated land protection. It primarily involves simulating and forecasting future land use changes to develop strategies to safeguard cultivated land. The model can improve the comprehension of various demands for cultivated land and ways to preserve it, thereby offering a scientific basis for decision-making.

NIS (natural increase scenario): This scenario serves as a foundation for other projections, assuming that natural disasters or significant national policies and regulations will not substantially influence future land use changes in Xinjiang. This scenario also assumes that each land use type will continue to change following historical trends.

EDS (economic development scenario): Given that Xinjiang's overall economic strength is relatively weak and its economic development lags, the central challenge for its future progress remains how to achieve economic advancement. This pivotal issue encompasses the potential for growth within Xinjiang, focusing on fostering economic expansion and optimizing economic benefits. Hence, the future land demand in Xinjiang should be strategically planned to cater to socio-economic development needs. It includes ways to safeguard ecologically important lands under continual economic development.

EPS (ecological protection scenario): In Xinjiang, ecological land conservation is crucial for comprehensive ecological safeguarding. The forthcoming development of the arid northwestern region must ensure the protection, restoration, and enhancement of the terrestrial ecosystem sustainability. Future planning and development in Xinjiang should focus on maximizing its ecosystem service value, emphasizing prioritizing ecological benefits.

We refer to reference [51] for different social and economic development goals and government development plans. The four scenarios described above are set up as follows: (1) NIS assumes that land use changes in 2020−2050 are not affected by major policies and plans, and that the magnitude and trend of future land use changes continue the evolution and development pattern of the 2000−2020 period. The land use raster number for the next 30 years under the natural development scenario is obtained by running the CA-Markov transfer probability matrix to obtain the number of land use grids under the natural development scenario. (2) CLP: Based on the natural development scenario, cultivated land is protected according to the "Outline of the National Overall Land Use Plan (2006−2020) (https://www.gov.cn/guoqing/2008-10/24/content_2875234.htm, accessed on 24 October 2008)" and "Overall Land Use Plan of the Xinjiang Uygur Autonomous Region (2006−2020) (https://zrzyt.xinjiang.gov.cn/xjgtzy/ghjh/201806/3036bbc523c0456cb43e41cd27e8bd06.shtml, accessed on 23 June 2018)" to ensure that cultivated land area occupies a larger proportion in each land use category, and cultivated land will increase by 1.2 times compared to the natural development scenario. (3) EPS prioritizes ecological benefits, ensuring the quantitative advantages of the ecological land types of woodland, grassland, and watershed, and restricting their large-scale and high-rate transformation to other land types. Compared to the natural development scenario, the woodland, grassland, and watershed areas have increased by 1.2, 1.2, and 1.6 times, respectively. (4) EDS: Based on the natural development scenario, economic development is reasonably guided and controlled according to relevant planning policies such as Xinjiang Uygur Autonomous Region New Urbanization Plan (2014−2020) (https://xjdrc.xinjiang.gov.cn/xjfgw/c108364/202108/1f41aafc062c4c10af324d0ba42f4c44.shtml, accessed on 30 August 2021) and Xinjiang Uygur Autonomous Region Town System Plan (2021−2035) (https://www.gov.cn/gongbao/2024/issue_11386/202406/content_6955759.html, accessed on 17 April 2024). Compared to the natural development scenario, the urban construction land area will grow moderately. However, disorderly expansion will be strictly controlled to avoid excessive conversion to other land types, such as arable and forest land. Compared to the natural development scenario, cultivated land, forest land, grassland, and water areas have increased by 1.2, 1.2, 1.6, and 1.2 times, respectively.

We utilized the InVEST-PLUS model to incorporate LUCC data from Xinjiang covering 2000 to 2020, aiming to evaluate the fluctuations in carbon storage. We used different scenarios for simulation in Xinjiang from 2020 to 2050, such as the CLP, NIS, EPS, and EDS. Subsequently, we predicted carbon storage from 2030 to 2050. The study's research framework, methods, and procedures are depicted in Figure 2.

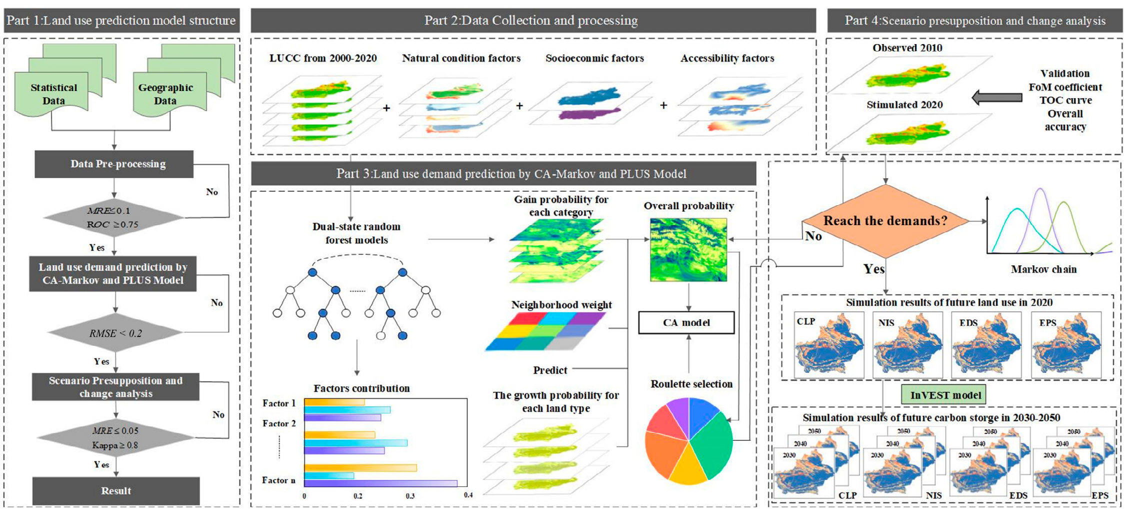

Figure 2. This study employs a flowchart to illustrate its methodology.

3. Results

3.1. Analyzing Carbon Storage Under LUCC

3.1.1. LUCC Characteristics in Xinjiang

Figure 3 shows the land use remote sensing monitoring data for 2000, 2005, 2010, 2015, and 2020, based on which we calculated a land use transfer matrix. Supplementary Table S1 shows the decline in forest, grassland, and unused land in 2000−2020 by 626.92, 13,786.30, and 7700.77 km^2, respectively. In contrast, cultivated land, water, and construction land increased by 18,072.56, 855.4, and 3186.03 km^2, respectively. For the past twenty years, the land use transfer has occupied 28,546.57 km^2. The significant changes primarily involved the grassland donor converting to the cultivated land recipient. Cultivated land, the dominant beneficiary, had an inflow about 11 times higher than the outflow (19,834.37 km^2 vs. 1761.8 km^2). Construction land received an inflow of 3189.01 km^2, and cultivated land was the main donor, contributing 822.87 km^2. The forest outflow (995 km^2) was slightly higher than the inflow (368.07 km^2). The forest outflow mainly became cultivated land (830.22 km^2), but a small amount of forest originated from cultivated land (54.71 km^2). Unused land had a slightly lower outflow (866.46 km^2) than inflow (8567.23 km^2), while it also originated from cultivated land (41 km^2). In addition, the area of water transfer was small, without an obvious transfer pattern.

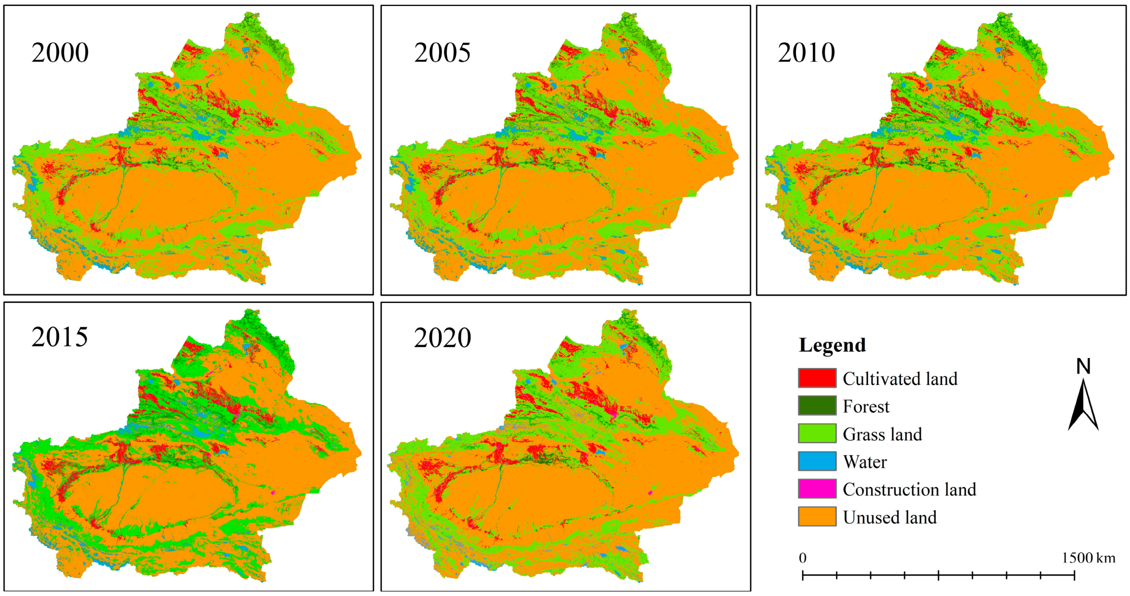

Figure 3. The LULC maps for 2000, 2005, 2010, 2015, and 2020.

Regarding transfers between land use types (Supplementary Figure S1), they mainly included the Altai Mountains, the north and south slopes of the Tianshan Mountains, Ili Valley, the north and south parts of the Tarim Basin, and the forest area of the Kunlun Mountains. The Tianshan Mountain region was the most important area regarding the transition from arable land to building land. There was a relatively large conversion of forest to cultivated land in the Tianshan Mountains. Moreover, forest to grassland occurred mainly in the Tarim Basin. Interestingly, the conversion of unused land to other land use types was relatively high and concentrated in all five major regions. Other conversions, including forest to cultivated land, construction land to water, and construction land to grassland, predominantly occurred in scattered patch patterns. The conversion of forests and grasslands to cultivated land was more serious, occurring mainly on the northern and southern slopes of the Tianshan Mountains and in the northern and southern parts of the Tarim Basin. The transfer of unused land to other categories was also notably significant, primarily focused in the following key areas: the Altai Mountains, the northern and southern slopes of the Tianshan Mountains, the Ili Valley, the northern and southern parts of the Tarim Basin, and the forests of the Kunlun Mountains. Other transfer types were small and insignificant. These included converting forest land to construction land, arable land to water bodies, and construction land to grassland, typically as small, scattered, and dispersed patches.

The Sankey diagram was plotted to quantify the flow and diversity of land use changes and depict the overall distribution of land use changes in 2000–2020 (Figure 4). The period witnessed many conversions of grassland and unused land, where grassland was mainly converted to unused land, cropland, and forest, and unused land was mainly converted to grassland and cultivated land. The largest conversions involved cultivated land to grassland, forest to grassland, and water to unused land. Adopting five-year intervals, land use transfers occurred mainly in 2015–2020.

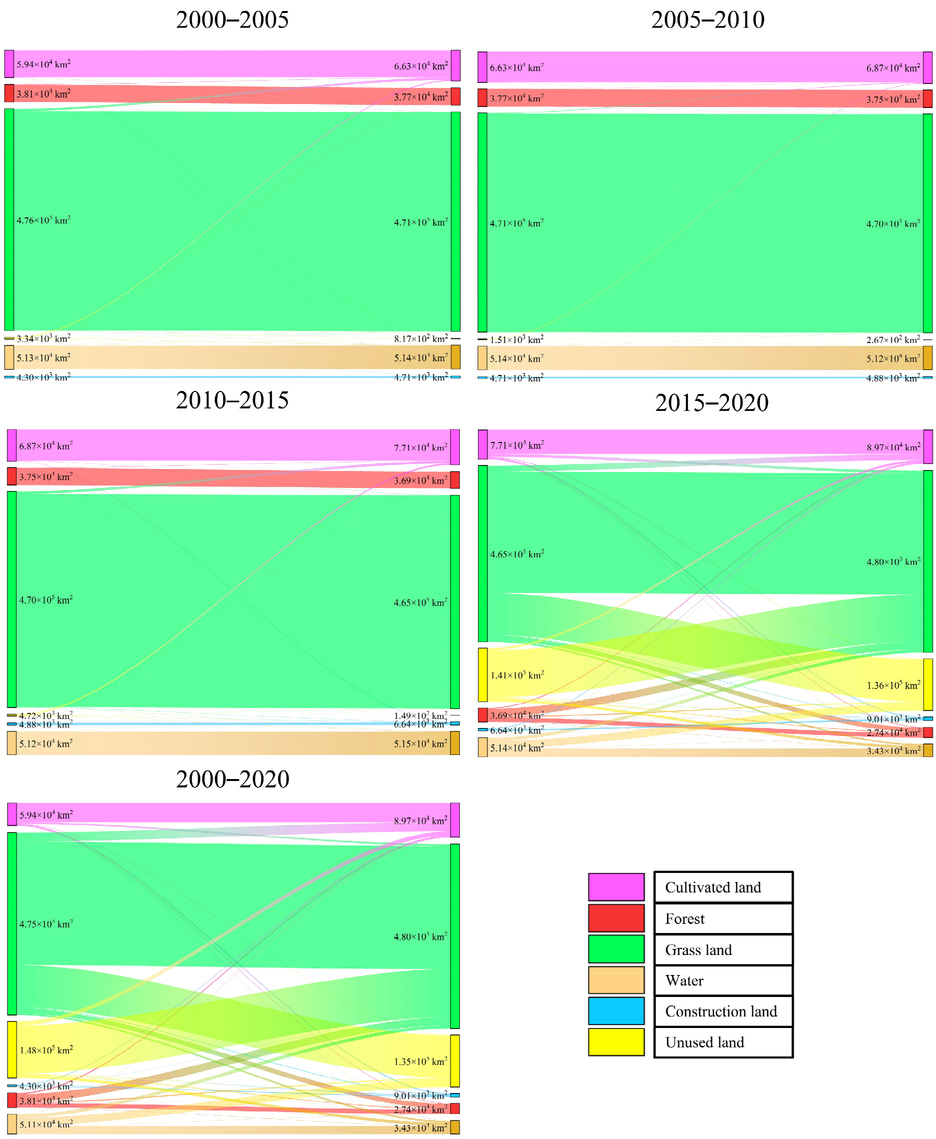

Figure 4. Land use conversions in Xinjiang from 2000 to 2020.

3.1.2. Dynamics of Carbon Storage in 2000−2020

The calculated carbon storage changes only referred to converted areas, and unconverted areas were excluded. The most significant carbon storage variations occurred in areas used for construction and agriculture. The carbon storage in Xinjiang in 2000–2020 were 85.69×10^8, 85.79×10^8, 85.87×10^8, 86.01×10^8, and 86.71×10^8 t, and the carbon density values were 52.55, 52.62, 52.67, 52.76, and 52.77 t/hm^2, respectively. Over the past two decades, aggregate changes in carbon storage were insignificant, increasing to 1.01×10^8 t and decreasing carbon density by 0.22 t/hm^2. The 2000–2020 period recorded a total decrease of 9.7% in carbon storage, which increased by 0.1×10^8, 0.08×10^8, 0.14×10^8, and 0.7×10^8 t, while carbon density decreased by 1.03, 0.07, 0.05, and 0.01 t/hm^2 in 2000–2005, 2005–2010, 2010–2015, and 2015–2020, respectively (Table 3).

Table 3. Impacts of land use change on carbon storage in Xinjiang from 2000 to 2020 ($\times 10^8$ t).

Year	Cultivated Land	Forest	Grassland	Water	Construction Land	Unused Land
2000	52.31	1.77	0.31	26.05	3.77	1.48
2005	52.27	1.77	0.33	25.86	4.11	1.46
2010	52.25	1.77	0.34	25.83	4.24	1.46
2015	52.16	1.79	0.44	25.45	4.73	1.45
2020	52.49	1.86	0.48	25.68	4.75	1.46

Carbon storage across Xinjiang maintained a relatively steady spatial configuration from 2000 to 2020 (Figure 5). Carbon source areas were mainly in the Altai Mountains (a-1)–(e-1), Tianshan Mountains (b-1)–(b-5), Yili Valley (c-1)–(c-5), Kunlun Mountains (e-1)–(e-5), and the outer edge of the oasis in the Tarim Basin (d-1)–(d-5). These areas were situated close to locations with strong economic activities and frequent land use conversions, making it difficult to form carbon sinks. On the other hand, carbon sinks were mainly located in unused desert and Gobi areas, resulting in less pronounced carbon storage changes. Low carbon storage was predominantly found in mountainous areas, water bodies (lakes), and urban construction sites. Medium carbon storage was primarily found in desert areas with harsh environments along mountain ranges, basins, and river valleys. High carbon storage was concentrated mainly in high-elevation mountain forest areas.

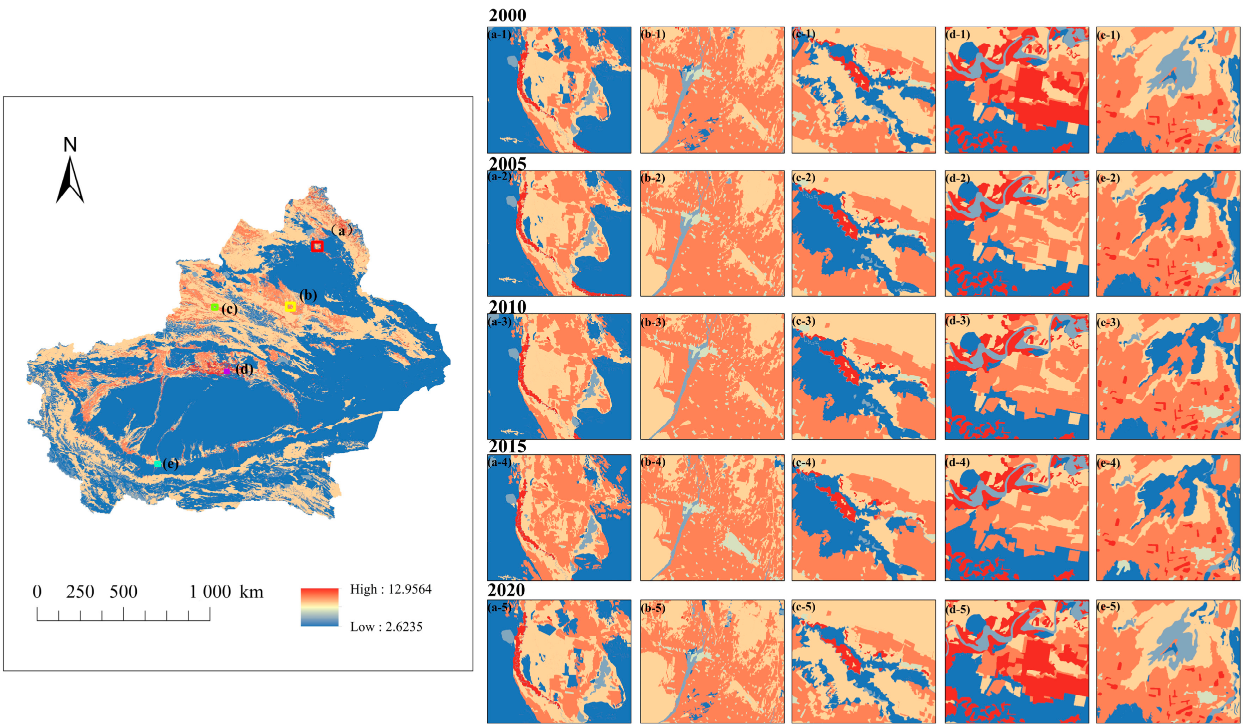

Figure 5. Spatial and temporal distribution of carbon storage in Xinjiang from 2000 to 2020: (**a-1**–**a-5**) Altai Mountains, (**b-1**–**b-5**) Tianshan Mountains, (**c-1**–**c-5**) Ili Valley, (**d-1**–**d-5**) Kunlun Mountains, and (**e-1**–**e-5**) Tarim Basin.

3.1.3. Choosing the Most Suitable Grid Scale Using Binary Logistic Regression

The factors shaping land use in Xinjiang were intricate and varied. The drivers should be judiciously assessed to enhance the predictive precision of the PLUS model and simulation results. LUCC was complex, requiring different drivers for various regions and times. Therefore, driver selection should follow some guiding principles, consult the literature, and consider actual situations in Xinjiang. In Xinjiang, eleven factors that drive LUCC were selected based on natural, socio-economic, and accessibility criteria (Table 1) based on the following considerations: (1) consistency of factor data; (2) quantifiability of factors; (3) significant spatial differences and correlations; and (4) completeness of factor selection [62,63]. The layout of the specific determinants is shown in Supplementary Figure S2.

This research employed binary logistic regression, which surpasses traditional logistic regression in terms of accuracy [64]. The model was implemented for each land use category from 2000 to 2020, and ROC curves were used to test the drivers' statistical significance. Considering previous research findings and Xinjiang's realities, in this study, logistic regressions were conducted on eleven drivers of six land use types at five regional scales: 1000 m $\times$ 1000 m, 2000 m $\times$ 2000 m, 3000 m $\times$ 3000 m, 4000 m $\times$ 4000 m, and 5000 m $\times$ 5000 m. The results of this study are summarized below. The ROC values for each land use type at different scales are presented in Supplementary Table S2. In light of the results, the best simulation scale was determined to be 4000 m $\times$ 4000 m, the regression coefficient file was established, and the simulation was conducted.

3.2. Accuracy Validation of the Markov-PLUS Model

This study enlisted the Markov model to conduct simulations. The simulated values were compared against the actual ones to determine the relative error rate. Supplementary Table S3 presents results indicating relative error rates of about 1%, which implies a close agreement between real-world conditions and forecasted outcomes. To verify the model's precision, the 2010 and 2020 land use data in Xinjiang were used as the first and last period data, respectively. Nine indicators were selected as driving factors to obtain the development probability of each category through the LEAS module. Using the development probability results, the CARS module was applied to simulate the spatial distribution of land use in 2020 based on the 2010 land use data. The simulated outcomes for 2020 LUCC were compared with the actual LUCC data for that year. The Kappa coefficient acquired through precision validation was 0.8. The excellent simulation outputs and accuracy suggested that the model could be employed to reliably predict future LUCC distribution in Xinjiang. However, policy factors could have a significant influence on land use changes. Future studies should consider integrating quantitative policy indicators into model calculations to improve the accuracy of predictions.

3.3. Forecasting Upcoming Land Use Distributions Using the PLUS Model

3.3.1. Analyzing Carbon Stock Changes Under Four Scenarios in 2030−2050

Using the Markov and PLUS models and a land use conversion matrix, we forecasted the future land use configurations of Xinjiang under CLP, the NIS, EDS, and EPS in 2020−2050 (Figure 6). The simulated land use and carbon storage data are summarized in Table 4. By combining our findings with previous studies, valuable insights were obtained.

Using the LUCC data from 2020, the Markov model predicted LUCC in 2030−2050 under various scenarios (Figure 6). There will be a continued decline in cropland, forests, and water resources by 2050 under the CLP scenario compared to 2030, with a reduction of 708.48 km^2, 1539.18 km^2, and 25,034.76 km^2 in cultivated land, respectively. Regarding the transfer direction, grassland, construction, and unused land will be reduced by 4263.75 km^2, 22,329.18 km^2, and 689.49 km^2, respectively (Figure 7). In the future, forests will mainly be converted to grassland; grasslands will change into cultivated land, forest, water, and construction land. Under CLP, the projected land use change trends from 2020 to 2050 are similar to 2000−2020.

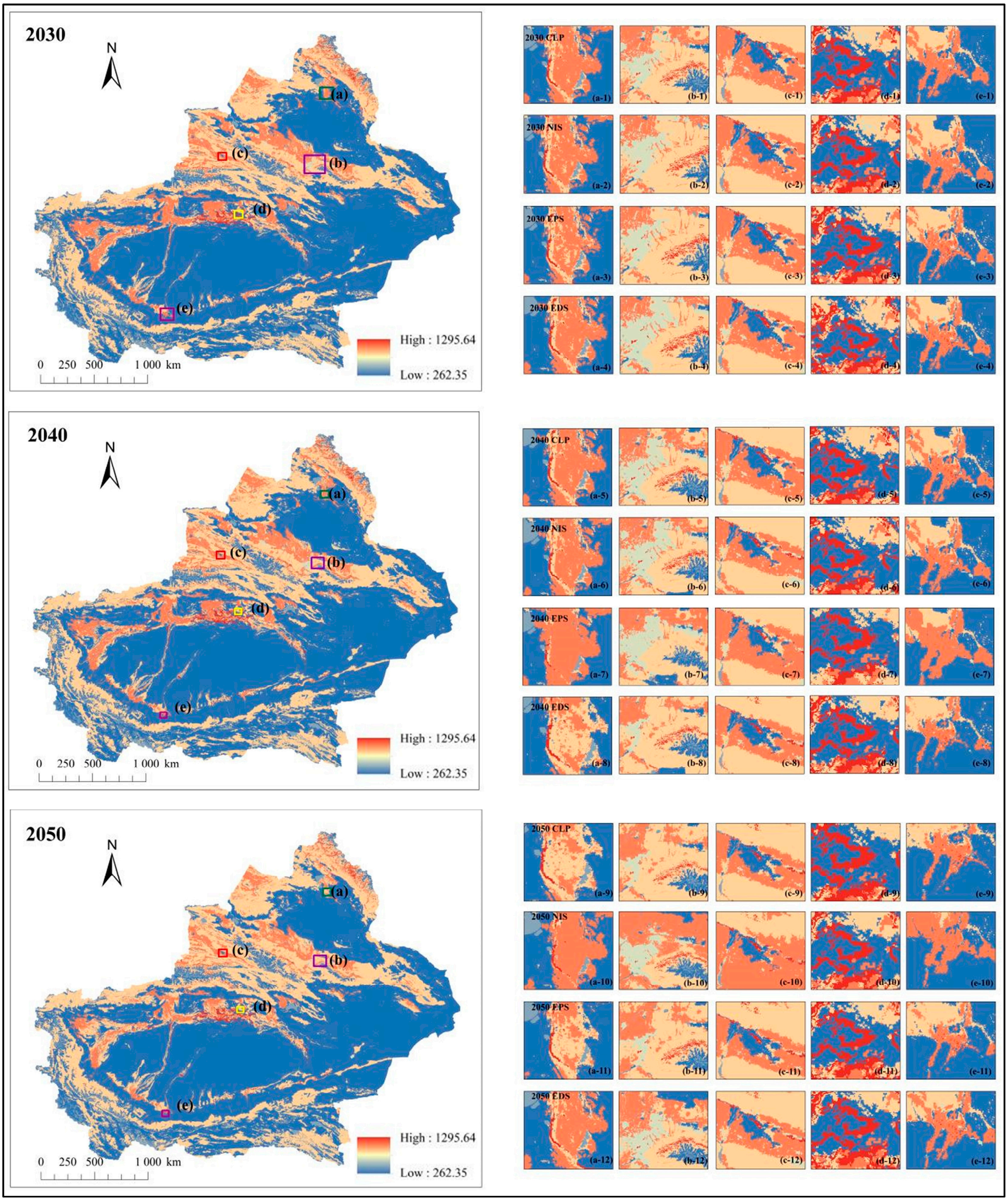

Figure 6. The alteration in carbon storage distribution throughout the Xinjiang region is projected from 2020 to 2050. Notes: (**a-1**–**a-12**) Altai Mountains', (**b-1**–**b-12**) Tianshan Mountains, (**c-1**–**c-12**) Ili Valley, (**d-1**–**d-12**) Kunlun Mountains, and (**e-1**–**e-12**) Tarim Basin. Note: Different color codes represent scenario changes more distinctly, allowing for a clearer visualization of carbon storage trends.

Table 4. Estimates of the fluctuation in carbon storage due to LUCC from 2030 to 2050 under various scenarios ($\times 10^6$ t).

Scenario	Land Use Type					
	Cultivated Land	Forest	Grassland	Water	Construction Land	Unused Land
2030 CLP	51.86	1.94	0.41	25.23	5.30	1.38
2030 NIS	51.86	1.94	0.41	25.23	5.30	1.38
2030 EPS	51.93	1.90	0.48	25.47	4.88	1.45
2030 EDS	51.91	1.85	0.59	25.15	5.18	1.40
2040 CLP	51.93	1.85	0.63	25.07	5.18	1.45
2040 NIS	51.94	1.85	0.59	25.09	5.21	1.45
2040 EPS	50.92	1.94	0.56	25.74	5.38	1.27
2040 EDS	51.88	1.86	0.59	25.20	5.23	1.40
2050 CLP	52.00	1.90	0.20	26.22	4.23	1.41
2050 NIS	51.83	2.02	0.18	26.52	4.11	1.34
2050 EPS	51.99	1.85	0.59	25.19	5.19	1.40
2050 EDS	52.63	1.87	0.60	25.50	5.25	1.42

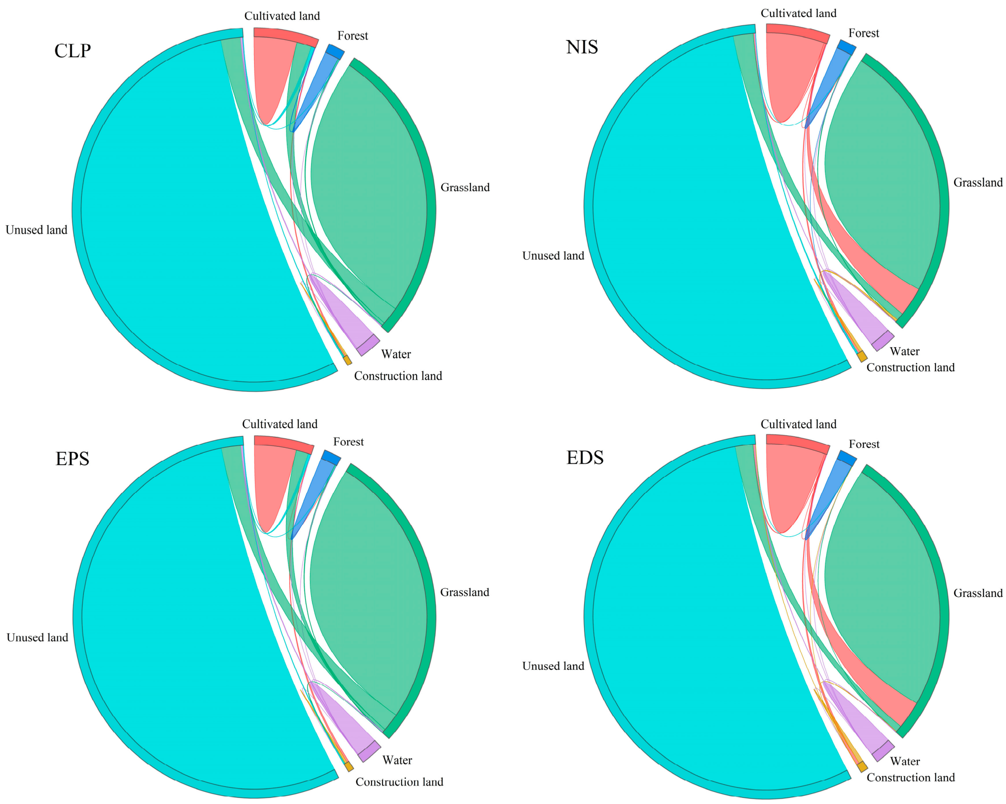

Figure 7. Chord diagrams illustrating the projected LUCC changes in Xinjiang from 2020 to 2050 (unit km^2).

Under the NIS, cultivated land and unused land will decrease by 2050 compared to 2020. Cultivated land, grassland, water, and unused land are projected to decrease by 69 km^2, 2102.67 km^2, 27,129.24 km^2, and 606.42 km^2, respectively. Forested area and construction land will expand by 1727.01 km^2 and 48,527.01 km^2, respectively (Figure 6). Concerning the land transfer direction (Figure 7), The bi-directional conversion between cultivated land and grassland will persist, with the transformation of cultivated land into unused land continuing to be predominant. The increase in the built-up land will mainly originate from arable land, grassland, and unused land, in addition to the fact that unused land will be mostly converted into arable land and grassland.

Under the EPS, the reductions in cultivated land, grassland areas, and construction land are 921.96 km^2, 5583.96 km^2, and 14,345.1 km^2, respectively. On the other hand, the expanse of forest, water, and unutilized lands expands by 1368.45 km^2, 18,992.16 km^2, and 490.41 km^2, respectively (Figure 6). This means that implementing ecological conservation efforts and expanding forest areas are key to enhancing carbon stock. However, under the existing conditions, the only way to ensure arable land holdings and the demand for land for construction is to upgrade large tracts of grassland and unused land to forest, while at the same time expanding the water bodies. Regarding spatial distribution, the pattern mirrors that of the NIS, but compared with it, the number of areas with high carbon density increases.

In the accelerated EDS, the increase in unused land is more significant than in the NIS. The area of forest cover has been significantly reduced to 862.1 km^2. Meanwhile, there is only a slight rise in other land areas, the reduction in farmland is not as pronounced as in the NIS, and the increase in unused land is transformed by land types other than cultivated land. The decrease in carbon storage is smaller than in the NIS, but the difference in the total change amount is insignificant. Comparative analyses indicate that despite the constraints of a very rapid EDS aimed at limiting and accelerating land expansion for construction, the difference in the spatial distribution of the total amount of land is not significantly different from that of the NIS.

3.3.2. Impact of Land Use Change on Carbon Storage

Throughout the five intervals of 2000, 2005, 2010, 2015, and 2020, it was noted that carbon storage in Xinjiang's six major land types generally exhibited a trend towards stabilization (Table 3). Regarding alterations in LUCC, cultivated land and water comprised 61% and 29% of the mean total carbon storage, respectively. Construction land accounted for 5.4%, while forests and unused lands had the smallest contributions. The land use results in 2030 were projected for CLP, the NIS, EPS, and EDS, for which the carbon storage in Xinjiang for 2030 was 86.11 $\times$ 10^8, 86.07 $\times$ 10^8, 86.01 $\times$ 10^8, and 86.11 $\times$ 10^8, respectively, and the carbon densities were 52.9, 52.88, 52.9, and 52.9 $Mg{\cdot}hm^{-2}$, respectively. For 2040, the carbon storage was 86.12 $\times$ 10^8, 86.15 $\times$ 10^8, 85.80 $\times$ 10^8, and 85.96 $\times$ 10^8, and the carbon densities were 52.91, 52.93, 52.71, and 52.81 $Mg{\cdot}hm^{-2}$. For 2050, the carbon storage was 86 $\times$ 10^8, 87.26 $\times$ 10^8, 86.2 $\times$ 10^8, 87.38 $\times 10^8$, and 87.38 $\times$ 10^8, respectively, and the carbon densities were 52.84, 53.61, 52.96, and 53.68 $Mg{\cdot}hm^{-2}$, respectively.

Compared with 2000, the four scenario projections for 2030 will generate an increase in total carbon storage by 0.42 $\times$ 10^8 t (CLP), 0.38 $\times 10^8$ t (NIS), 0.41 $\times$ 10^8 t (EPS), and 0.42 $\times$ 10^8 t (EDS) (Table 4). Compared with 2000, in 2040, the total carbon storage will increase by 0.44 $\times$ 10^8 t (CLP), 0.46 $\times$ 10^8 t (NIS), 0.11 $\times$ 10^8 t (EPS), and 0.27 $\times$ 10^8 t (EDS). Compared with 2000, in 2050, the total carbon storage will increase by 0.31 $\times$ 10^8 t (CLP), 1.58 $\times$ 10^8 t (NIS), 0.51 $\times$ 10^8 t (EPS), and 1.69 $\times$ 10^8 t (EDS).

Among the various LUCC types, cultivated land constituted the largest carbon pool, representing an average of 61% of the cumulative carbon storage. The other LUCC types followed in descending order of carbon storage, namely water > forest > unused land > construction land > grassland. Compared to 2020, there was a net growth in carbon storage within forests, grasslands, and construction lands in 2030. In contrast, arable land, water, and unused land decreased. Geospatially, the regions with high carbon density in Xinjiang tended to spread, maintaining a distribution pattern largely similar to that of 2020. Furthermore, the total carbon storage for the four scenarios in 2040 and 2050 showed an upward trajectory. Cropland remained the largest carbon pool among the different LUCC types, and the order of carbon storage for the other LUCC types remained unchanged. Additionally, carbon intensity increased in 2050 compared to 2040 for all four scenarios, showing a general uptrend from 2030 to 2050.

Under the CLP scenario, the transformations in cultivated land and grassland resemble those of the NIS, and construction land will diminish compared to the NIS. The cultivated land increase is attributed to conversion from water and unused land. These changes imply that restrictions on construction land expansion can protect cultivated land, contrasting with a sharp cultivated land decline under the NIS. Compared to 2020, carbon storage is expected to decline by 0.6×10^8 t in 2030. In addition, the total carbon storage across the four scenarios in 2040 and 2050 will be reduced by 0.61×10^8 and 0.5×10^8 t, respectively, compared with 2020. This result indicates an improvement over the NIS due to reduced forest land leading to carbon losses.

Under the NIS, the shifts in land use categories between 2030 and 2050 will parallel those observed from 2000 to 2020. By 2030, a substantial reduction in cultivated land is anticipated, whereas an increase is expected in grasslands, water, and particularly in built-up areas. The conversion of cultivated land to construction land remains the primary land use alteration. Accordingly, the carbon stocks in Xinjiang's arable land, forests, watersheds, and unused land will be reduced by 0.58×10^8, 0.02×10^8, 0.53×10^8, and 0.06×10^8 t, respectively, and the total carbon stock will be reduced by 0.64×10^8 t, respectively. By 2050, carbon storage in cultivated land, grassland and construction land will experience an increment of 0.01×10^8, 0.11×10^8, and 0.43×10^8 t, respectively. The decrease in cultivated land results in a decline in carbon storage by 0.65 t and 0.57 t in 2040 and 2050, respectively, compared to 2020 under the four considered scenarios.

Under the EPS, there will be a substantial rise in forest and water areas relative to the NIS. The forest expansion is mainly caused by conversion from cultivated land and grassland. The overall carbon storage will grow by 0.6×10^8 t compared to 2020. In addition, the cumulative carbon storage for the four scenarios is projected to fall by 0.92×10^8 and 0.51×10^8 t in 2040 and 2050, respectively, compared to 2020. The geographical distribution of carbon stocks remains consistent with the natural variability scenario, but there is an increase in areas of high carbon density compared to the natural variability scenario. This result implies that the advancement of ecological conservation practices and the augmentation of ecological components, including forests and aquatic systems, positively contribute to the carbon sequestration capacity of terrestrial ecosystems.

In contrast, there will be a less pronounced reduction in cultivated land compared to the NIS. Total carbon stocks are projected to decrease by 0.61×10^8 t, relatively smaller than the NIS, but the difference is insignificant. Furthermore, total carbon storage is projected to decrease by 0.75×10^8 t in 2040 and increase by 0.67×10^8 t in 2050 under the four scenarios, compared with 2020. Despite the constraints of fast economic development and accelerated construction land expansion, little difference from the NIS is observed. This result indicates that the region has undergone rapid urban economic development under the NIS.

Comparing the four scenarios, it is observed that CLP will have the largest carbon sink area in 2030, trailed by the EDS and EPS, while the NIS is the smallest. In 2040, the NIS will have the largest carbon sink area, followed by CLP and the EDS, while the EPS will be the smallest. In 2050, the EDS will have the largest carbon sink area, succeeded by the NIS and EPS, with CLP having the smallest. The key carbon sinks in Xinjiang are located in the Altai Mountains, the northern and southern slopes of the Tianshan Mountains, the Ili Valley, the northern and southern parts of the Tarim Basin, and the forested areas within the Kunlun Mountains. The carbon sinks significantly outnumber the carbon source areas, mainly in mountain ranges and places with abundant vegetation surrounding the basins. This pattern suggests the area's strong carbon storage capacity and stable ecological development.

3.3.3. Temporal and Spatial Dynamics of Carbon Storage in Response to Land Use Change

Figure 5 shows areas with carbon storage changes in 2000–2020. They are predominantly found in the northern Altai Mountains, the north and south slopes of the Tianshan Mountains, Ili Valley, Tarim Basin, and Kunlun Mountains. This pattern coincides with the distribution of high carbon storage, with intertwined and overlapping carbon source and sink areas in the northern foothills of the Tianshan Mountains and the periphery of the oases in the Tarim Basin. These areas are close to intense human and economic activities and frequent land use conversions that make it difficult to form carbon sinks. Significant alterations in carbon storage are discernible for the four land development scenarios projected from 2030 to 2050 (Table 4). This result suggests a change in carbon storage due to drivers, with an overall upward trend. In summary, the distribution of high-to-medium carbon storage across Xinjiang is mainly located in the middle, and low carbon storage across Xinjiang is closely linked to land use patterns and driving factors. Carbon storage is primarily found in dense vegetation surrounding mountain ranges and basins, indicating substantial regional carbon storage potential and a stable ecosystem state.

In Figure 8, the carbon stock hot spots under different scenarios in Xinjiang in 2030 are almost the same, and they are all distributed in the Aksu region in southern Xinjiang, and the cold spots are distributed in high-altitude alpine areas as well as in desert areas. The distribution of carbon stock hot spots under different scenarios in 2040 varies greatly, and Xinjiang's vast unutilized land area will become a carbon stock hot spot under CLP and the NIS. In the EPS, the carbon stock hot spots are located in forested areas; in the EDS, the carbon stock hot spots are very small in extent and almost disappear, except for some oasis and grassland areas. In 2050, the distribution of carbon stock hot spots under all scenarios will be small, with the hot spots under CLP and the EPS distributed in the form of patches in the oasis areas in southern Xinjiang and the grassland areas in the north, and the main hot spots under the NIS and EDS concentrated in the forested areas in northern Xinjiang, the grassland areas in the Yili, and the main oasis areas in the Ring Tarim Basin.

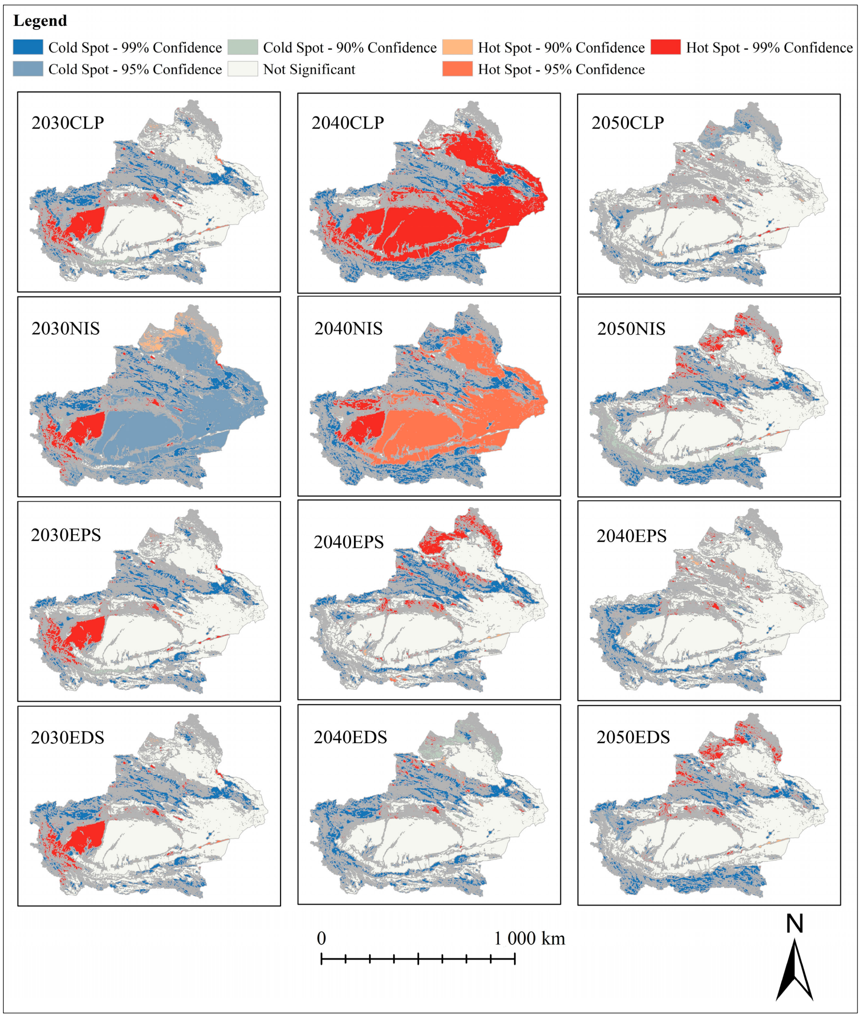

Figure 8. The hot and cold spots of carbon storage across CLP, the NIS, EPS, and EDS from 2030 to 2050.

4. Discussion

4.1. Carbon Storage Distribution Patterns Associated with Land Use

The validation results exhibit a strong alignment with the outcomes of earlier research. Our analysis found that low carbon storage is scattered around mountain ranges instead of deserts and undeveloped land such as the Gobi. This pattern is intimately connected to land use classifications, the mountainous terrain, and the distinct stratification of vegetation across the elevational gradient. The general landscape has a characteristic fabric, such as glaciers and snow at mountain tops, woodlands on mountain slopes, grasslands in the foothills, and urban development on gentle slopes of the valleys. This natural configuration has generated a carbon storage pattern anchored by mountain ranges to display a nested distribution of high and low values. The study area embodies beneficial carbon sinks in historical and future periods, but the arid climate and fragile ecology restrict its carbon sequestration capacity compared with humid regions. Therefore, studying the status of carbon sinks in Xinjiang and the northwest arid region is significant to China's achievement of carbon peaking and neutrality.

4.2. Constraints to Accurate Assessment of Carbon Storage

Given the intricate and changeable nature of LUCC, certain uncertainties in carbon storage distribution are inevitable. Initially, carbon storage simulations are significantly affected by LUCC. We selected 11 drivers. However, because of the limitations and parameter selection in the land use simulation model (PLUS), potential errors may arise in the final simulation results. Additionally, while the effects of policy and institutional elements on LUCC can be significant, they are challenging to measure quantitatively [50]. Secondly, changes in temperature, rainfall, altitude, and environmental conditions in different regions can affect carbon density and thus reduce the accuracy of carbon storage assessments. Thirdly, carbon storage was calculated using the PLUS-InVEST model, which ignores other factors, such as photosynthetic rate and soil microbial activity, which strongly influence carbon sinks [7]. Fourth, while some studies have examined the relative impact of LUCC and climate on terrestrial ecosystems, incorporating LUCC policies into diverse climate models remains a future challenge [65,66]. Consequently, our future research efforts will focus on a more comprehensive assessment of the impacts of land use change on ecosystem services and their cumulative effects. We will also explore the balance required between multiple ecosystem services under different potential future scenarios [67]. Future research could also further explore the dynamic impact of factors like microbial activity and soil characteristics on carbon storage, improving the precision of carbon stock assessments.

4.3. Policy Implications

This research selected Xinjiang as our study area due to its extensive land area and natural limitations typical of China's northwest arid region. Additionally, it is situated at the core area of the Belt and Road national policy with a high development potential. Xinjiang is undergoing rapid urbanization, posing significant challenges to sustaining terrestrial ecosystem services [68]. Estimating forthcoming changes in LUCC and their potential ecological consequences under various developmental scenarios aids in comprehending and mitigating these effects. However, a decline in carbon storage has occurred, predominantly due to the degradation of grasslands. Considering that carbon stocks will decrease under the CLP scenario, Xinjiang should appropriately limit the expansion of cultivated land and reduce the encroachment of cultivated land into forest land in the future. CLP is the scenario with the largest future increase in carbon stocks. Therefore, it is essential to expand ecological restoration initiatives like converting cultivated land back to forest and grassland [69], and the "Three North Shelter Forests" program [70]. Diverse afforestation methods can be combined with tree irrigation and grassland to enhance carbon sequestration capacity. The government can conduct more research to improve ecological restoration and increase carbon sinks in the ecosystem. In order to cope with changes in carbon storage under different scenarios, it is recommended that layered and regionalized ecological protection and land management strategies be adopted in accordance with the ecological characteristics and land use status of different regions. This includes implementing targeted ecosystem restoration measures in specific regions and optimizing land use practices (returning farmland to forests, afforestation, land salinization management, wind and sand stabilization, etc.) to enhance the carbon storage capacity of soil and vegetation. In addition, systematic carbon stock monitoring and land use scenario simulation projections can provide a scientific basis for carbon neutralization targets under different ecological environments. This will ultimately lead to a sustained increase in carbon stocks and promote the realization of the regional carbon neutrality goal, while at the same time facilitating sustainable ecological protection and economic development.

5. Conclusions

From the findings, the following conclusion can be made:

Within this investigation, we modeled the prospective LUCC and alterations in ecosystem carbon storage in Xinjiang, China, spanning the 2020−2050 period across four diverse developmental scenarios. We accomplished this by establishing an integrated framework that amalgamates the Markov, InVEST, and PLUS models to precisely simulate shifts in carbon reserves under varying scenarios. The forecasted land use transformations are contingent upon the four simulated climate scenarios. The framework of this research provides innovative perspectives that can assist decision-makers in their management choices and support China in reaching its "carbon neutrality" objective while enhancing ecosystem services in additional urban areas.

Carbon storage experienced a continuous and steady rise in 2000−2020, with a net increase of 1.03×10^8 t. Compared to 2020, carbon storage in the three developmental scenarios projected for 2050 will substantially increase. Carbon storage decreased by a small amount of 0.71×10^8 under the CLP scenario, while the NIS, EDS, and EPS increased the carbon storage by 6.37×10^8, 7.78×10^8, and 8.49×10^8 t, respectively. The study demonstrated that carbon storage simulations under different scenarios could understand the underlying factors and limitations and offer hints to achieve sustainable development in Xinjiang and other similar places. Future research can assess district-specific scenarios, improve analytical methods, and develop a more objective evaluation of terrestrial ecosystems.

The study area has sustained or created some carbon sinks, which can be further improved for carbon storage. Nonetheless, compared with the humid southern regions, the capacity for carbon sequestration in the sink areas of Xinjiang is restricted by its arid climate and fragile ecology. Even though the ecosystems in arid zones are more susceptible to damage, the impacts of LUCC are often overlooked due to the common misconception that their ecosystems are less active and, hence, less susceptible to damage. Ignoring human disruptions on the carbon cycle in the northwest arid region may lead to mistaken decisions and actions. A detailed analysis of the human impacts on ecosystems and the carbon cycle should dispel this misunderstanding.

Compared to the southern humid region of China, Xinjiang's ecosystem carbon sequestration capacity is relatively limited due to its arid climate, which is not conducive to the growth of large plants or dense vegetation. Consequently, this study offers pertinent contributions to the comprehensive appraisal of carbon storage at the county level. Nevertheless, additional investigations are warranted to expand on these outcomes due to constraints in land use/land cover classification techniques, driving factors, model precision, and carbon density parameters.

Supplementary Materials: The following supporting information can be downloaded at: https://www.mdpi.com/article/10.3390/rs16234439/s1, Figure S1: Analysis of the spatial dynamics of land-use changes in Xinjiang from 2000 to 2020: (a) Altai Mountains, (b) Tianshan Mountains, (c) Ili Valley, (d) Kunlun Mountains, and (e) Tarim Basin; Figure S2: Spatial patterns of the LUCC drivers in Xinjiang; Table S1: Land-use transition matrix in Xinjiang from 2000 to 2020 (×102 km2); Table S2:

ROC at different scales; Table S3: The outcome of the Markov prediction and corresponding deviation ($\times10^4$ km^2).

Author Contributions: Conceptualization, J.S. and X.H.; methodology, J.S. and X.H.; software, J.S. and X.H.; formal analysis, J.S. and X.H.; investigation, J.S., X.H. and F.Z.; resources, J.S., X.H. and F.Z.; data curation, J.S. and X.H.; writing—original draft, X.H. and J.S.; writing—review and editing, J.S., X.H., F.Z., X.M. and C.Y.J.; visualization, C.Y.J., B.A.J. and N.W.C.; supervision, X.H. and F.Z.; project administration, F.Z.; funding acquisition, F.Z. All authors have read and agreed to the published version of the manuscript.

Funding: This research was supported by the Key Research and Development Program of the Xinjiang Uygur Autonomous Region (2022B01012) and the Tianshan Talent Project (Phase III) of the Xinjiang Uygur Autonomous Region.

Data Availability Statement: The data presented in this study are available on request from the corresponding author.

Acknowledgments: We acknowledge and appreciate the contribution of anonymous reviewers and editors in appraising our manuscript and offering helpful comments.

Conflicts of Interest: The authors declare no conflicts of interest.

References

1. Field, C.B.; Barros, V.R. (Eds.) *Climate Change 2014–Impacts, Adaptation and Vulnerability: Regional Aspects*; Cambridge University Press: Cambridge, UK, 2014.
2. Masson-Delmotte, V.; Zhai, P.; Pörtner, H.-O.; Roberts, D.; Skea, J.; Shukla, P.R.; Pirani, A.; Moufouma-Okia, W.; Péan, C.; Pidcock, R.; et al. Global Warming of 1.5 °C. An IPCC Special Report on the Impacts of Global Warming of 1.5 °C above Pre-industrial Levels and Related Global Greenhouse Gas Emission Pathways. In *The Context of Strengthening the Global Response to the Threat of Climate Change, Sustainable Development, and Efforts to Eradicate Poverty*; IPCC: Geneva, Switzerland, 2019; Volume 1, pp. 93–174.
3. Zhu, L.; Song, R.; Sun, S.; Li, Y.; Hu, K. Land use/land cover change and its impact on ecosystem carbon storage in coastal areas of China from 1980 to 2050. *Ecol. Indic.* **2022**, *142*, 109178. [CrossRef]
4. Ito, A.; Nishina, K.; Noda, H.M. Impacts of future climate change on the carbon budget of northern high-latitude terrestrial ecosystems: An analysis using ISI-MIP data. *Polar Sci.* **2016**, *10*, 346–355. [CrossRef]
5. Rodrigues, C.I.D.; Brito, L.M.; Nunes, L.J. Soil carbon sequestration in the context of climate change mitigation: A review. *Soil Syst.* **2023**, *7*, 64. [CrossRef]
6. Wang, J.N.; Zhang, Z. Land use change and simulation analysis in the northern margin of the Qaidam Basin based on Markov-PLUS model. *J. Northwest For. Univ.* **2022**, *37*, 139–148.
7. Mustard, J.F.; Defries, R.S.; Fisher, T.; Moran, E. Land-use and land-cover change pathways and impacts. In *Land Change Science: Observing, Monitoring and Understanding Trajectories of Change on the Earth's Surface*; Springer: Dordrecht, The Netherlands, 2012; pp. 411–429.
8. Zhang, M.; Huang, X.; Chuai, X.; Yang, H.; Lai, L.; Tan, J. Impact of land use type conversion on carbon storage in terrestrial ecosystems of China: A spatial-temporal perspective. *Sci. Rep.* **2015**, *5*, 10233. [CrossRef]
9. Tian, L.; Tao, Y.; Fu, W.; Li, T.; Ren, F.; Li, M. Dynamic simulation of land use/cover change and assessment of forest ecosystem carbon storage under climate change scenarios in Guangdong Province, China. *Remote Sens.* **2022**, *14*, 2330. [CrossRef]
10. Xie, L.; Bai, Z.; Yang, B.; Fu, S. Simulation Analysis of Land-Use Pattern Evolution and Valuation of Terrestrial Ecosystem Carbon Storage of Changzhi City, China. *Land* **2022**, *11*, 1270. [CrossRef]
11. Liu, X.; Wang, S.; Wu, P.; Feng, K.; Hubacek, K.; Li, X.; Sun, L. Impacts of urban expansion on terrestrial carbon storage in China. *Environ. Sci. Technol.* **2019**, *53*, 6834–6844. [CrossRef]
12. Hoque, M.Z.; Islam, I.; Ahmed, M.; Hasan, S.S.; Prodhan, F.A. Spatio-temporal changes of land use land cover and ecosystem service values in coastal Bangladesh. *Egypt. J. Remote Sens. Space Sci.* **2022**, *25*, 173–180.
13. Sippel, S.; Reichstein, M.; Ma, X.; Mahecha, M.D.; Lange, H.; Flach, M.; Frank, D. Drought, heat, and the carbon cycle: A review. *Curr. Clim. Change Rep.* **2018**, *4*, 266–286. [CrossRef]
14. Zheng, H.; Zheng, H. Assessment and prediction of carbon storage based on land use/land cover dynamics in the coastal area of Shandong Province. *Ecol. Indic.* **2023**, *153*, 110474. [CrossRef]
15. Yu, G.; Zhu, J.; Xu, L.; He, N. Technological approaches to enhance ecosystem carbon sink in China: Nature-based solutions. *Bull. Chin. Acad. Sci.* **2022**, *37*, 490–501. (In Chinese)
16. Zhang, S.; Bai, X.; Zhao, C.; Tan, Q.; Luo, G.; Wu, L.; Xi, H.; Li, C.; Chen, F.; Ran, C.; et al. China's carbon budget inventory from 1997 to 2017 and its challenges to achieving carbon neutral strategies. *J. Clean. Prod.* **2022**, *347*, 130966. [CrossRef]
17. Yang, F.; He, F.; Li, S.; Li, M.; Wu, P. A new estimation of carbon emissions from land use and land cover change in China over the past 300 years. *Sci. Total Environ.* **2023**, *863*, 160963. [CrossRef]

18. Li, Y.; Liu, W.; Feng, Q.; Zhu, M.; Yang, L.; Zhang, J.; Yin, X. The role of land use change in affecting ecosystem services and the ecological security pattern of the Hexi Regions, Northwest China. *Sci. Total Environ.* **2023**, *855*, 158940. [CrossRef]
19. Wei, H.; Xiong, L.; Tang, G.; Strobl, J.; Xue, K. Spatial–temporal variation of land use and land cover change in the glacial affected area of the Tianshan Mountains. *Catena* **2021**, *202*, 105256. [CrossRef]
20. Li, Z.T.; Li, M.; Xia, B.C. Spatio-temporal dynamics of ecological security pattern of the Pearl River Delta urban agglomeration based on LUCC simulation. *Ecol. Indic.* **2020**, *114*, 106319. [CrossRef]
21. Zhou, J.; Zhao, Y.; Huang, P.; Zhao, X.; Feng, W.; Li, Q.; Xue, D.; Dou, J.; Shi, W.; Wei, W.; et al. Impacts of ecological restoration projects on the ecosystem carbon storage of inland river basin in arid area, China. *Ecol. Indic.* **2020**, *118*, 106803. [CrossRef]
22. Zhao, B.; Kreuter, U.; Li, B.; Ma, Z.; Chen, J.; Nakagoshi, N. An ecosystem service value assessment of land-use change on Chongming Island, China. *Land Use Pol.* **2004**, *21*, 139–148. [CrossRef]
23. Zhang, S.; Fan, W.; Li, Y.; Yi, Y. The influence of changes in land use and landscape patterns on soil erosion in a watershed. *Sci. Total Environ.* **2017**, *574*, 34–45. [CrossRef]
24. Wu, L.; Zhang, X.; Hao, F.; Wu, Y.; Li, C.; Xu, Y. Evaluating the contributions of climate change and human activities to runoff in typical semi-arid area, China. *J. Hydrol.* **2020**, *590*, 125555. [CrossRef]
25. Xu, X.; Jiao, F.; Liu, H.; Gong, H.; Zou, C.; Lin, N.; Xue, P.; Zhang, M.; Wang, K. Persistence of increasing vegetation gross primary production under the interactions of climate change and land use changes in Northwest China. *Sci. Total Environ.* **2022**, *834*, 155086. [CrossRef] [PubMed]
26. Li, Y.; Yao, S.; Jiang, H.; Wang, H.; Ran, Q.; Gao, X.; Ding, X.; Ge, D. Spatial-temporal evolution and prediction of carbon storage: An integrated framework based on the MOP-PLUS-InVEST model and an applied case study in Hangzhou, East China. *Land* **2022**, *11*, 2213. [CrossRef]
27. Huang, C.; Zhou, Y.; Wu, T.; Zhang, M.; Qiu, Y. A cellular automata model coupled with partitioning CNN-LSTM and PLUS models for urban land change simulation. *J. Environ. Manag.* **2024**, *351*, 119828. [CrossRef]
28. Chen, C.; Liu, J.; Bi, L. Spatial and temporal changes of habitat quality and its influential factors in China based on the InVEST model. *Forests* **2023**, *14*, 374. [CrossRef]
29. Li, P.; Chen, J.; Li, Y.; Wu, W. Using the InVEST-PLUS model to predict and analyze the pattern of ecosystem carbon storage in Liaoning Province, China. *Remote Sens.* **2023**, *15*, 4050. [CrossRef]
30. He, Y.; Ma, J.; Zhang, C.; Yang, H. Spatio-temporal evolution and prediction of carbon storage in Guilin based on FLUS and InVEST models. *Remote Sens.* **2023**, *15*, 1445. [CrossRef]
31. Zhu, J.; Hu, X.; Xu, W.; Shi, J.; Huang, Y.; Yan, B. Regional carbon stock response to land use structure change and multi-scenario prediction: A case study of Hunan province, China. *Sustainability* **2023**, *15*, 12178. [CrossRef]
32. Yu, Y.; Guo, B.; Wang, C.; Zang, W.; Huang, X.; Wu, Z.; Xu, M.; Zhou, K.; Li, J.; Yang, Y. Carbon storage simulation and analysis in Beijing-Tianjin-Hebei region based on CA-plus model under dual-carbon background. *Geomat. Geomat. Nat. Hazards Risk* **2023**, *14*, 2173661. [CrossRef]
33. Li, Q.; Chen, Y.; Shen, Y.; Li, X.; Xu, J. Spatial and temporal trends of climate change in Xinjiang, China. *J. Geogr. Sci.* **2011**, *21*, 1007–1018. [CrossRef]
34. Wang, Z.; Wu, B.; Ma, Z.; Zhang, M.; Zeng, H. Distinguishing natural and anthropogenic contributions to biological soil crust distribution in China's drylands. *Sci. Total Environ.* **2024**, *907*, 168009. [CrossRef] [PubMed]
35. Xu, L.; He, N.; Yu, G. A dataset of carbon density in Chinese terrestrial ecosystems (2010s). *China Sci. Data* **2019**, *4*, 90–96. [CrossRef]
36. Chuai, X.; Huang, X.; Lai, L.; Wang, W.; Peng, J.; Zhao, R. Land use structure optimization based on carbon storage in several regional terrestrial ecosystems across China. *Environ. Sci. Policy* **2013**, *25*, 50–61. [CrossRef]
37. Chen, G.S.; Yang, Y.S.; Jie, J.S.; Du, Z.X.; Zhang, J. Total belowground carbon allocation in China's forests. *Acta Ecol. Sin* **2007**, *27*, 5148–5157.
38. Alam, S.A.; Starr, M.; Clark, B.J. Tree biomass and soil organic carbon densities across the Sudanese woodland savannah: A regional carbon sequestration study. *J. Arid. Environ.* **2013**, *89*, 67–76. [CrossRef]
39. Kuzyakov, Y. Priming effects: Interactions between living and dead organic matter. *Soil Biol. Biochem.* **2010**, *42*, 1363–1371. [CrossRef]
40. Okolo, C.C.; Gebresamuel, G.; Retta, A.N.; Zenebe, A.; Haile, M. Advances in quantifying soil organic carbon under different land uses in Ethiopia: A review and synthesis. *Bull. Natl. Res. Cent.* **2019**, *43*, 1–24. [CrossRef]
41. Xie, X.L.; Sun, B.; Zhou, H.Z.; Li, Z.P.; Li, A.B. Estimation and spatial distribution analysis of soil organic carbon density and storage in China. *Acta Pedol. Sin.* **2004**, *1*, 35–43.
42. Cui, D.; Li, Y.L.; Wang, X.Y.; Zhao, X.Y.; Zhang, T.H. Spatial distribution of aboveground biomass of grassland in desert and desertified regions in northern China. *J. Desert Res.* **2011**, *31*, 868–872.
43. Shoemaker, D.A.; BenDor, T.K.; Meentemeyer, R.K. Anticipating trade-offs between urban patterns and ecosystem service production: Scenario analyses of sprawl alternatives for a rapidly urbanizing region. *Comput. Environ. Urban Syst.* **2019**, *74*, 114–125. [CrossRef]
44. Lu, Y.; Xu, X.; Li, J.; Feng, X.; Liu, L. Research on the spatio-temporal variation of carbon storage in the Xinjiang Tianshan Mountains based on the InVEST model. *Arid. Zone Res.* **2022**, *39*, 1896–1906.

45. Wang, Y.; Luo, G.; Zhao, S.; Han, Q.; Li, C.; Fan, B.; Chen, Y. Effects of arable land change on regional carbon balance in Xinjiang. *Acta Geogr. Sin.* **2014**, *69*, 110–120.
46. Hua, L.; Zhiqiang, B.; Yue, F.; Fan, Z.; Yanliang, H. Spatial Pattern of Forest Carbon Storage and Carbon Density in the Kanas National Natural Reserve. *J. Landsc. Res.* **2015**, *7*, 38.
47. Aishan, T.; Betz, F.; Halik, Ü.; Cyffka, B.; Rouzi, A. Biomass carbon sequestration potential by riparian forest in the Tarim River Watershed, Northwest China: Implication for the mitigation of climate change impact. *Forests* **2018**, *9*, 196. [CrossRef]
48. Jia, X.; Jia, L.; Ye, J.; Fei, B.; Bao, F.; Xu, X.; Zhang, L.; Wu, B. Estimating carbon storage of desert ecosystems in China. *Int. J. Digit. Earth* **2023**, *16*, 4113–4125.
49. Zhang, J.; Li, M.; Ao, Z.; Deng, M.; Yang, C.; Wu, Y. Estimation of soil organic carbon storage of terrestrial ecosystem in arid western China. *J. Arid Land Resour. Environ.* **2018**, *42*, 335–344. [CrossRef]
50. Wang, N.; Chen, X.; Zhang, Z.; Pang, J. Spatiotemporal dynamics and driving factors of county-level carbon storage in the Loess Plateau: A case study in Qingcheng County, China. *Ecol. Indic.* **2022**, *144*, 109460. [CrossRef]
51. Han, M.; Xu, C.; Long, Y.; Liu, F. Simulation and prediction of changes in carbon storage and carbon source/sink under different land use scenarios in Arid Region of Northwest China. *Bull. Soil Water Conserv.* **2022**, *42*, 335.
52. Zhu, G.; Qiu, D.; Zhang, Z.; Sang, L.; Liu, Y.; Wang, L.; Zhao, K.; Ma, H.; Xu, Y.; Wan, Q. Land-use changes lead to a decrease in carbon storage in arid region, China. *Ecol. Indic.* **2021**, *127*, 107770. [CrossRef]
53. Mansour, S.; Al-Belushi, M.; Al-Awadhi, T. Monitoring land use and land cover changes in the mountainous cities of Oman using GIS and CA-Markov modelling techniques. *Land Use Pol.* **2020**, *91*, 104414. [CrossRef]
54. Gidey, E.; Dikinya, O.; Sebego, R.; Segosebe, E.; Zenebe, A. Cellular automata and Markov Chain (CA_Markov) model-based predictions of future land use and land cover scenarios (2015–2033) in Raya, northern Ethiopia. *Model. Earth Syst. Environ.* **2017**, *3*, 1245–1262. [CrossRef]
55. Fu, X.; Wang, X.; Yang, Y.J. Deriving suitability factors for CA-Markov land use simulation model based on local historical data. *J. Environ. Manag.* **2018**, *206*, 10–19. [CrossRef] [PubMed]
56. Tang, L.; Ke, X.; Zhou, T.; Zheng, W.; Wang, L. Impacts of cropland expansion on carbon storage: A case study in Hubei, China. *J. Environ. Manag.* **2020**, *265*, 110515. [CrossRef] [PubMed]
57. Babbar, D.; Areendran, G.; Sahana, M.; Sarma, K.; Raj, K.; Sivadas, A. Assessment and prediction of carbon sequestration using Markov chain and InVEST model in Sariska Tiger Reserve, India. *J. Clean. Prod.* **2021**, *278*, 123333. [CrossRef]
58. Wu, H.; Yu, L.; Shen, X.; Hua, F.; Ma, K. Maximizing the potential of protected areas for biodiversity conservation, climate refuge and carbon storage in the face of climate change: A case study of Southwest China. *Biol. Conserv.* **2023**, *284*, 110213. [CrossRef]
59. Liang, Y.; Hashimoto, S.; Liu, L. Integrated assessment of land-use/land-cover dynamics on carbon storage services in the Loess Plateau of China from 1995 to 2050. *Ecol. Indic.* **2021**, *120*, 106939. [CrossRef]
60. Guo, H.; Cai, Y.; Li, B.; Tang, Y.; Qi, Z.; Huang, Y.; Yang, Z. An integrated modeling approach for ecological risks assessment under multiple scenarios in Guangzhou, China. *Ecol. Indic.* **2022**, *142*, 109270. [CrossRef]
61. Gao, L.; Tao, F.; Liu, R.; Wang, Z.; Leng, H.; Zhou, T. Multi-scenario simulation and ecological risk analysis of land use based on the PLUS model: A case study of Nanjing. *Sustain. Cities Soc.* **2022**, *85*, 104055. [CrossRef]
62. Xiang, S.; Wang, Y.; Deng, H.; Yang, C.; Wang, Z.; Gao, M. Response and multi-scenario prediction of carbon storage to land use/cover change in the main urban area of Chongqing, China. *Ecol. Indic.* **2022**, *142*, 109205. [CrossRef]
63. Tao, Y.; Li, F.; Wang, R.; Zhao, D. Effects of land use and cover change on terrestrial carbon stocks in urbanized areas: A study from Changzhou, China. *J. Clean. Prod.* **2015**, *103*, 651–657. [CrossRef]
64. Luo, T.; Tan, R.; Kong, X.; Zhou, J. Analysis of the driving forces of urban expansion based on a modified logistic regression model: A case study of Wuhan City, Central China. *Sustainability* **2019**, *11*, 2207. [CrossRef]
65. Mahmood, R.; Pielke Sr, R.A.; Hubbard, K.G.; Niyogi, D.; Bonan, G.; Lawrence, P.; McNider, R.; McAlpine, C.; Etter, A.; Gameda, S. Impacts of land use/land cover change on climate and future research priorities. *Bull. Am. Meteorol. Soc.* **2010**, *91*, 37–46. [CrossRef]
66. Pielke, R.A.; Pitman, A.; Niyogi, D.; Mahmood, R.; McAlpine, C.; Hossain, F.; Goldewijk, K.K.; Nair, U.; Betts, R.; Fall, S.; et al. Land Use/Land Cover Changes and Climate: Modeling Analysis and Observational Evidence. *Wiley Interdiscip. Rev. Clim. Chang.* **2011**, *2*, 828–850. [CrossRef]
67. Li, Z.; Cheng, X.; Han, H. Future impacts of land use change on ecosystem services under different scenarios in the ecological conservation area, Beijing, China. *Forests* **2022**, *11*, 584. [CrossRef]
68. Shi, M.; Wu, H.; Jiang, P.; Shi, W.; Zhang, M.; Zhang, L.; Zhang, H.; Fan, X.; Liu, Z.; Zheng, K.; et al. Cropland expansion mitigates the supply and demand deficit for carbon sequestration service under different scenarios in the future—The case of Xinjiang. *Agriculture* **2022**, *12*, 1182. [CrossRef]

69. Temperton, V.M.; Buchmann, N.; Buisson, E.; Durigan, G.; Kazmierczak, Ł.; Perring, M.P.; de Sá Dechoum, M.; Veldman, J.W.; Overbeck, G.E. Step back from the forest and step up to the Bonn Challenge: How a broad ecological perspective can promote successful landscape restoration. *Restor. Ecol.* **2019**, *27*, 705–719. [CrossRef]
70. Cao, S.; Suo, X.; Xia, C. Payoff from afforestation under the three-North shelter forest program. *J. Clean Prod.* **2020**, *256*, 120461. [CrossRef]